GeoStudio Example File
Parameterizing the SANICLAY Model

To see the latest GeoStudio learning content, visit Seequent Learning Centre and search the catalogue for “GeoStudio”.

Introduction

This example demonstrates how to parameterize the SANICLAY constitutive model from laboratory data. The parameters are then used in numerical simulations of the laboratory tests and the simulated results are compared with the reference paper and the measured data.

Formulation

A brief overview of the SANICLAY model is provided as a prerequisite to the parameterizing procedure. Details of the formulation are presented in the SIGMA/W reference book (Seequent ULC, 2024). This document refers to the formulation in triaxial stress space where p' and q denote the mean effective stress and deviatoric stress, respectively as:

$$p' = (\sigma'_a + 2\sigma'_r)/3 \qquad \text{Equation 1}$$

$$q = \sigma_a - \sigma_r \qquad \text{Equation 2}$$

here $\sigma'_a \; and \; \sigma'_r$ stand for the axial and the radial effective stresses, respectively.

Note the following points about anisotropic loading, as shown in Figure 1:

1. Any loading encompassing a deviatoric component in triaxial stress space initiates a rotated elliptical yield surface with the gradient of β. For isotropic loadings, $\beta = 0$.
2. Along a stress path with a constant stress ratio, such as K_0 loading ($\eta = \eta_{k0}$), the yield surface ceases to rotate but keeps expanding due to the increase of the size of the yield surface (p'_0) along the path. The blue ellipse shows the yield surface associated with the initial stresses, while the green ellipse illustrates it at the end of the K_0 loading.
3. The stress-strain response associated with 1-D (K_0) loading, is assumed linear in $e - \ln p'$ space.

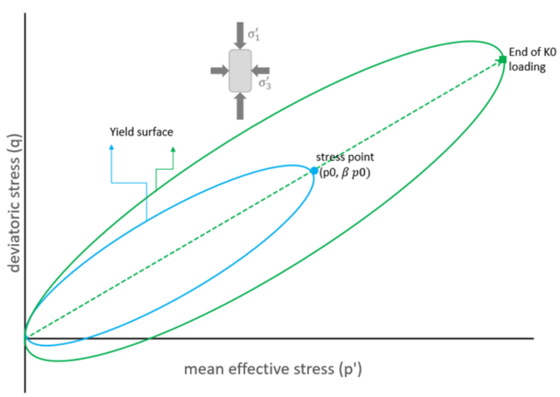

Figure 1. SANICLAY: response to anisotropic compression.

Note the following points about unloading, as shown in Figure 2:

1. Unloading causes the stress path to track inside the latest yield locus (green elliptical surface) until reaching it (blue diamond point). As the stress path touches the latest yield surface, the yield surface evolves and orients with updated β and p'_0. The red ellipse represents the yield surface at the end of the unloading. Note to the changes in the gradient and the size of the yield surface on the right side graphs.

2. 1-D (K_0) unloading produces a stress-strain response that follows the slope κ in $e - \ln p'$ space.

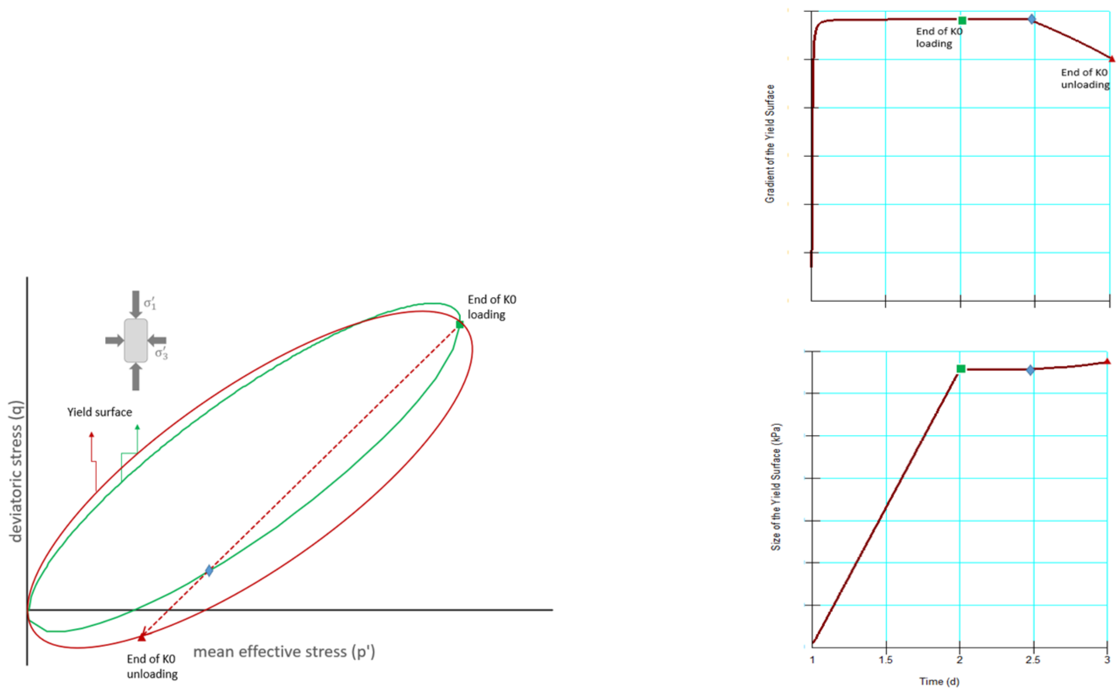

Figure 2. SANICLAY in triaxial stress space: response to a deviatoric unloading condition.

Figure 3 shows the yield surface (bold gray rotated ellipse) at the beginning of the undrained triaxial shearing path for a NC soil consolidated under K0 condition. The yield surface at the failure point is shown by the blue ellipse. Note the following in reference to Figure 3:

1. The SANICLAY material model is a critical-state-based constitutive model, meaning that under shearing, the critical state will eventually be reached, irrespective of specific stress paths.
2. The slope of the critical state line will be interpolated between the reference values M_c and M_e using the Lode angle. M_c and M_e denote the critical stress ratio in compression and extension, respectively.
3. The yield surface is a rotated ellipse that passes through the origin and intersects the stress ratio N at its peak point.
4. The model is non-associative. The plastic potential surface is also a rotated elliptical surface, defined by the gradient and size of the plastic potential surface (α and p'_α).
5. The overconsolidation ratio is the ratio between the maximum vertical effective stress experienced by the sample and the current vertical effective stress the sample is subjected to.
6. For a stress state inside the yield surface, the stress-strain response is elastic, and the bulk and shear moduli are both proportional to the mean effective stress, p' and the specific volume, $1 + e$.
7. After reaching the yield surface and as it rotates while rescales, the sample response becomes elastic-plastic. Incremental strains in this condition are the summation of elastic and plastic strains and so the current stress ratio plays a key role in the sample response.

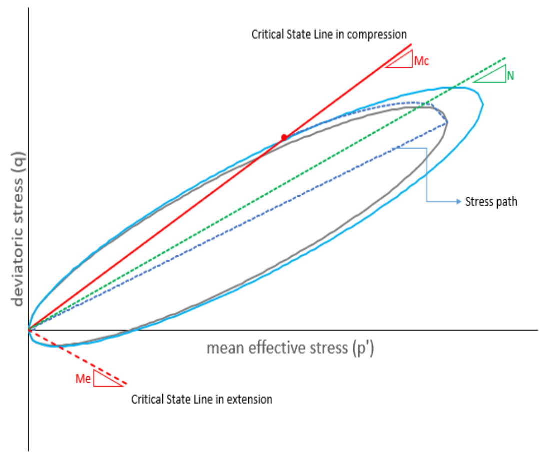

Elliptical yield function

$$f = (q - p'.\beta)^2 - (N^2 - \beta^2)p'(p'_0 - p') = 0$$

Elastic incremental strains

$$d\varepsilon_v^e = \frac{dp'}{K} \qquad K = \frac{p'(1+e)}{\kappa}$$

$$d\varepsilon_q^e = \frac{dq}{3G} \qquad G = \frac{3K(1-2\nu)}{2(1+\nu)}$$

Elliptical plastic potential function

$$g = (q - p'.\alpha)^2 - (M^2 - \alpha^2)p'(p_\alpha - p') = 0$$

Plastic incremental strains

$$d\varepsilon_v^p = \langle L \rangle p'(M^2 - \eta^2)$$

$$d\varepsilon_q^p = \langle L \rangle 2p'(\eta - \alpha)$$

Figure 3. SANICLAY model in triaxial stress space: key components of the formulation.

Regarding the rotational hardening options for the SANICLAY model in SIGMA/W note the main features as below:

1. In SANICLAY with RH 2013, the yield surface is defined by N which is not a constant value as it is in RH 2006. In the new version, N will be interpolated between the reference values N_c and N_e using the Lode angle. N_c and N_e denote the value of N in compression and extension, respectively.
2. In the SANICLAY with RH 2013 model, the inclination of the yield surface and the inclination of the plastic potential surface is considered with the same definition $(\beta = \alpha)$. Thus, the version has only one rotational hardening rule.

The state parameters of the model which include the gradient of the plastic potential surface (α), gradient of the yield surface size (β) and size of the yield surface (p'_0) can be monitored in SIGMA/W via Results/ Draw Graph/ Materia State Parameters window. The gradient of the yield and plastic potential surfaces are scalar representations of the tensors used to formulate and implement the model.

Table 1 lists the input parameters for both versions of the model.

Table 1. Input parameters for the SANICLAY model with RH 2006 and 2013.

Parameter	Dafalias et al. (2006)	Dafalias and Taiebat (2013)
	Symbol	
Compressibility of normally consolidated cl	λ	λ
Compressibility of overconsolidated clay	κ	κ
Poisson's ratio	ν	ν
Critical stress ratio in compression	M_c	M_c
Critical stress ratio in extension	M_e	M_e
Yield surface shape in compression	N	N_c
Yield surface shape in extension	N	N_e

Saturation limit of anisotropy	x	–
Rotational hardening parameter	–	s
Rotational hardening parameter	–	z
Rotational hardening parameter	–	Xi
Rate of evolution of anisotropy	C	C
Overconsolidation ratio	OCR	OCR
Earth pressure coefficient for normally compressed soil	$K_{0,nc}$	$K_{0,nc}$

Parameterization Procedure

Figure 4 provides a conceptual workflow for the model calibration procedure. For SANICLAY, the parameterization procedure is premised on the availability of triaxial test results for K_0-consolidated samples. The parameterization procedure produces the constants for the constitutive model. These constants are then used as inputs for the model when used in a numerical simulation. Finally, the parameterization is verified by comparing the simulated and measured results.

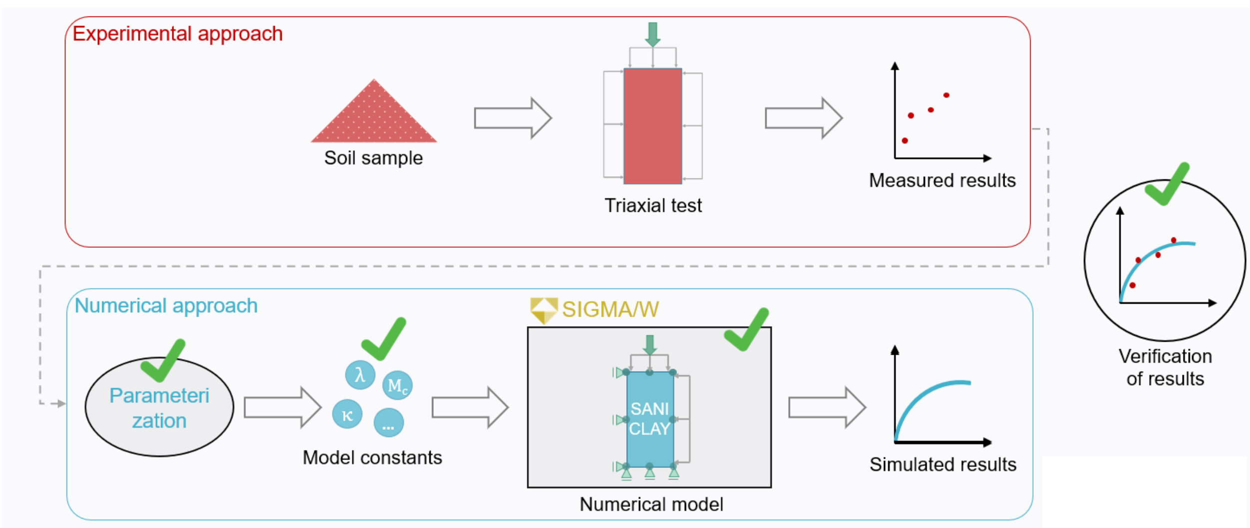

Figure 4. Conceptual workflow of the parameterization procedure.

In the subsequent sections the procedure of the determination of the model's parameter is presented. Note that only Step 4 defines the version specified parameters therefore all other steps are applicable for both versions of the model.

Step 1: Determine λ and κ

The first step is to determine the slope of the normal compression line λ and the slope of the unloading-reloading line κ (Figure 5). For this purpose, one-dimensional (K_0) consolidation or preferably isotropic consolidated tests using an oedometer or a triaxial device are required. Applied stresses must be significantly larger than the preconsolidation pressure and at least one unload-reload cycle needs to be done.

The trends of the measured values of p' and e during the loading portions of the graph can be fitted by a straight line with slope λ in both tests. Similarly, the measured values during the unloading cycle align along another line with slope κ. Therefore, the λ and κ parameters can be calculated directly using the method of least squares as below:

$$\lambda = -\frac{n\sum e \ln p' - \sum e \sum \ln p'}{n\sum (\ln p')^2 - [\sum \ln p']^2}$$ Equation 3

$$\kappa = -\frac{n\sum e_{ur} \ln p'_{ur} - \sum e_{ur} \sum \ln p'_{ur}}{n\sum (\ln p'_{ur})^2 - [\sum \ln p'_{ur}]^2}$$ Equation 4

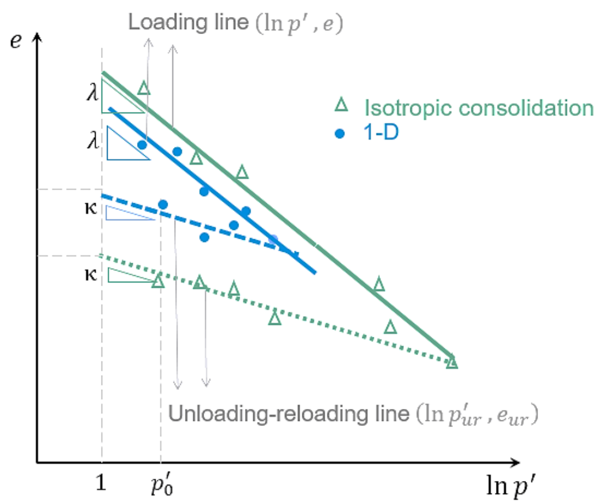

Figure 5. Determining the slopes λ *and* κ.

Step 2: Determine ν

The second step is to determine Poisson's ratio. As mentioned under Figure 2, the initial part of K_0-unloading path remains inside the yield surface and develops purely elastic strains. Considering the boundary condition of this path which implies $\delta\varepsilon_x = 0$, the measured strains follow:

$$\frac{\delta\varepsilon_v^e}{\delta\varepsilon_q^e} = \frac{3}{2}$$ Equation 5

From the elastic incremental strain equations (Figure 3), the slope of such a path is:

$$\frac{\delta q}{\delta p'} = \frac{3(1-2\nu)}{(1+\nu)}$$ Equation 6

Applying the method of least squares to the n measured (p', q) data sets along this path gives:

$$\frac{\delta q}{\delta p'} = \frac{n\sum qp' - \sum q \sum p'}{n\sum (p')^2 - \left[\sum p'\right]^2}$$ Equation 7

Combining Equation 7 and Equation 6 allows the calculation of ν.

Step 3: Determine M_c and M_e

The third step is to determine the critical state stress ratio M_c and M_e (Figure 6). According to critical state soil mechanics, stress paths of samples with different initial confining stresses eventually tend to the critical state at large deformation. Among the several possible setups, CK$_0$UC (undrained triaxial compression test on normally K_0-consolidated clay) and CK$_0$UE (undrained triaxial extension test on normally K_0-consolidated clay) setups are the best choices. Since the samples are sheared under the undrained condition, these tests are faster than drained tests and their results can be used to estimate other parameters later.

In both cases, the critical state line is a straight line that passes through failure points. Therefore, M_c and M_e is the slope of this line in the CK$_0$UC and CK$_0$UE test, respectively.

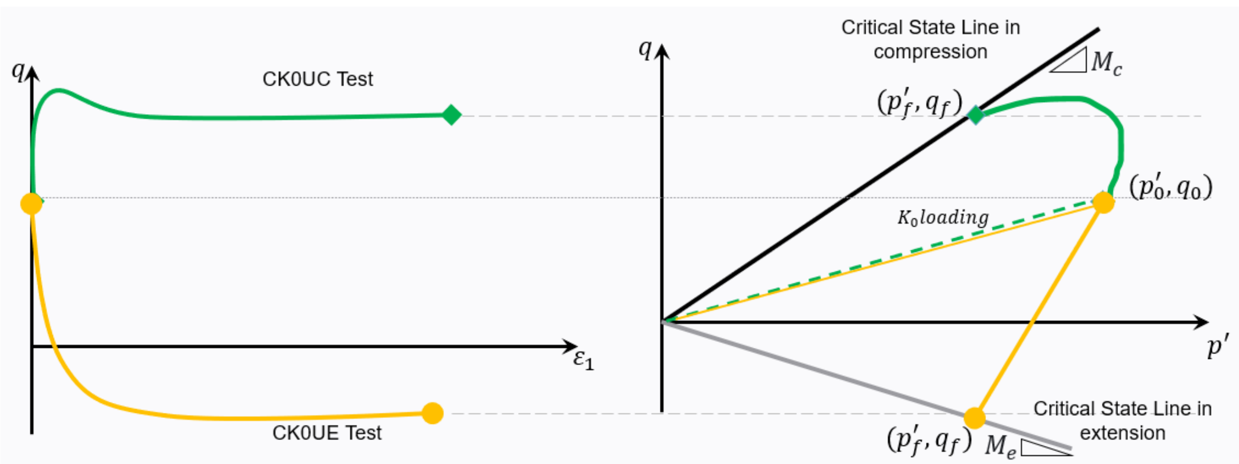

Figure 6. Determining the strength properties.

If more than one set of lab results is available, the corresponding critical stress ratio can be estimated by applying the method of least squares as shown below:

$$M_c = \frac{\sum p'_f q_f}{\sum p'^2_f}$$ Equation 8

$$M_e = -\frac{\sum p'_f q_f}{\sum p'^2_f}$$ Equation 9

Step 4: Version specified parameters

RH 2006: Determine N

The N parameter, which represents the shape of the yield surface can also be determined from a closed-form relationship using two pairs of data from a CK0UC test on normally consolidated samples.

The data used in Step 3: Determine M_c and M_e (CK$_0$UC) can be reused here, where the equation of the undrained stress path yields:

$$\frac{p'_f}{p'_{K0}} = \left(\frac{N^2 - \eta_{K0}^2}{N^2 - 2\eta_{K0}M_c + M_c^2}\right)^{1-\frac{\kappa}{\lambda}} \qquad \text{Equation 10}$$

where (p'_{K0}, η_{K0}) and (p'_f, M_c) refer to the data at the end of the K_0consolidation and at the critical state, respectively, as shown in Figure 7. Equation 10 can be easily solved for N.

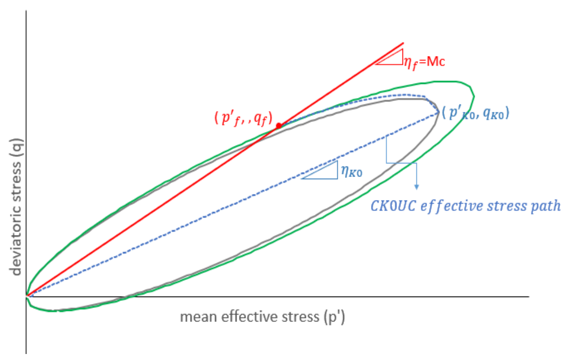

Figure 7. Effective stress path of the CK0UC test on NC sample.

The calculated N value from Equation 10 may need a slight adjustment if the C parameter takes a larger value than 8. In this case, the N parameter should be increased since the basic assumption of a non-rotating yield surface, on which Equation 10 is built, is no longer valid (see Dafalias *et al.*, 2006, for more details).

RH 2006: Determine x

The saturation limit of anisotropy (x) parameter can be determined using a closed-form relation with known values in a drained path with constant stress ratio, like the K_0-loading path in Figure 6. The relation is obtained from the hardening rule of the model and the boundary condition of the path as:

$$x = \frac{3\eta_{k0}\left(1 - \frac{\kappa}{\lambda}\right)}{\frac{3}{2}B{\eta_{k0}}^3 + {\eta_{k0}}^2 + \frac{3}{2}\eta_{k0}\left[2\left(1 - \frac{\kappa}{\lambda}\right) - BM_c^2\right] - M_c^2} \qquad \text{Equation 11}$$

where

$$B = -\frac{2(1+\nu)\kappa}{9(1-2\nu)\lambda} \qquad \text{Equation 12}$$

and

$$\eta_{k0} = 3(1 - K_0)/(1 + 2K_0) \quad \text{Equation 13}$$

where the K_0 is the measure value of the earth coefficient at rest. In absence of K_0 measurement, the parameter can be estimated from empirical relationships, such as:

$$K_0 = 1 - sin\phi \quad \text{Equation 14}$$

Where ϕ is the effective angle of shear resistance and can be calculated from M_c as:

$$\phi = Arcsin\left(\frac{3M_c}{6 + M_c}\right) \quad \text{Equation 15}$$

RH 2013: Determine S and Z

The K0 consolidation condition initially induces a simultaneous expansion and rotation of the PPS/YS towards a state where the stress ratio $\eta = q/p'$ and RH variable α acquire equilibrium values, while the PPS/YS continues to harden isotropically. Stated this, zeroing the rate of α yields a relation for determination of constant S and Z as:

$$\dot{\alpha} = 0 \rightarrow \alpha_{k0} = \pm \frac{M_c}{Z}\left\{1 - \exp\left[-S\left(\frac{|\eta_{k0}|}{M_c}\right)\right]\right\} \quad \text{Equation 16}$$

where

$$\alpha_{k0} = \frac{{\eta_{k0}}^2 + 3\eta_{k0}\left[1 - \frac{\kappa}{\lambda}\right] - {M_c}^2}{3\left(1 - \frac{\kappa}{\lambda}\right)} \quad \text{Equation 17}$$

and

$$\eta_{k0} = 3(1 - K_0)/(1 + 2 * K_0) \quad \text{Equation 18}$$

where the K_0 is the measure value of the earth coefficient at rest. Again, in absence of K_0 measurement, the parameter can be estimated from empirical relationships, such as Equation 14.

As shown by Dafalias and Taiebat (2013) one must have $S \leq Z$. With Adopting $Z = S$, as a very good default assumption, Equation 16 and Equation 17 suffice for determination of these parameters.

RH 2013: Determine N_c and N_e

Similar to the N parameter of RH 2006, the N_c parameter can be calculated from the undrained path in triaxial compression test on a K0 consolidated sample, CK_0UC, which has already been used for determination of M_c. Note that along this path, data of only two points are required: at the end of consolidation ($p'_{K_0}, \eta_{K_0}, \alpha_{K_0}$) and at critical state (p'_f, M_c, α_c). When these two pairs are inserted in the undrained stress path one has:

$$\frac{p'_f}{p'_{K0}} = \left[\frac{1 + \frac{\left(\eta_{K_0} - \alpha_{K_0}\right)^2}{\left(N_c^2 - \alpha_{K_0}^2\right)}}{1 + \frac{\left(M_c - \alpha_c\right)^2}{\left(N_c^2 - \alpha_c^2\right)}} \right]^{1 - \frac{\kappa}{\lambda}}$$

Equation 19

Where η_{K_0} and α_{K_0} can be calculated from Equation 17 and Equation 18, respectively and α_c:

$$\alpha_c = \frac{M_c}{Z}\left(1 - \exp\left(-S\right)\right)$$

Equation 20

Equation 19 can be easily solved for N_c.

To ensure that the SANICLAY with RH 2013 results in unique critical state line, the M and N must have a common Lode-angle dependent factor in their generalization to multiaxial stress space. Recall that in this version both M and N are interpolated between their reference values under the triaxial compression and triaxial extension conditions, using the Lode angle. This requirement introduces the following equation for determination of N_e parameter:

$$\frac{N_e}{N_c} = \frac{M_e}{M_c}$$

Equation 21

RH 2013: Determine Xi

This parameter prevents excessive rotation of the yield and plastic potential surfaces. The acceptable range of Xi is:

$$Xi \le -\frac{1}{S} ln\left(1 - Z\frac{min(M_e, N_e)}{M_c}\right)$$

Equation 22

A negative value of the quantity in the parentheses in Equation 22 implies that $Z > \frac{M_c}{min(M_e, N_e)}$. In this case, no remedy in terms of Xi is required. SIGMA/W checks out this condition internally and ignore the user defined value of Xi if no remedy is needed.

Step 5: Determine C

The calibration of parameter C requires trial simulation runs using all the other parameters already calibrated. This parameter quantifies the rate of rotation and distortion of the yield and plastic potential surfaces when plastic deformations occur. The most suitable test for calibrating the C parameter is a CK0UE test on normally consolidated sample, which has been already used in Step 3 to determine M_e. Considering the end of K_0-consolidation as the starting stress state of the test, in this test η_{in} is located far from η_f, therefore significant surface rotation is expected to happen (hence the correction on N proposed in the previous section). Note that the higher the value of C, the larger the predicted undrained strength in triaxial extension.

Step 6: Determine OCR

The last step is to determine the overconsolidation ratio OCR for each specimen (Figure 8). More specifically, the OCR is the ratio between the maximum vertical stress σ'_{max} that soil has ever experienced and the current vertical initial stress σ'_0.

$$OCR = \frac{\sigma'_{max}}{\sigma'_0} \quad \text{Equation 23}$$

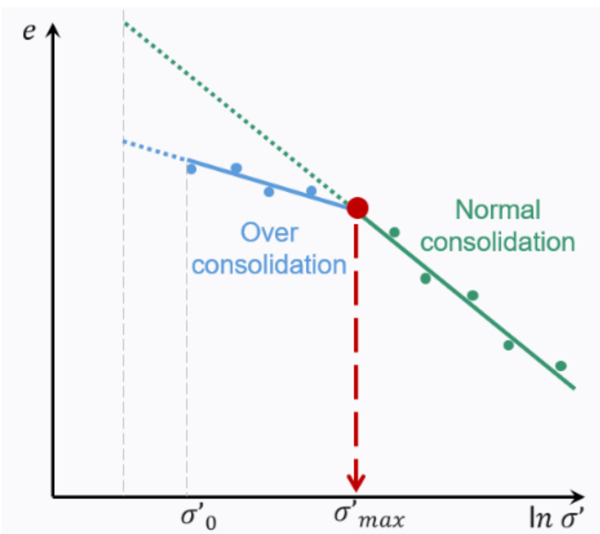

Figure 8. Determining the overconsolidation ratio OCR.

Application

Figure 9 to Figure 13 summarize the parameterization procedure as applied to the results of undrained triaxial tests on K_0-consolidated Lower Cromer Till (LCT) based on the work of Gens (1982). Table 2 provides a summary of the model input parameters obtained from the parameterization procedure, as well as the values proposed by Dafalias *et al.* (2006) and Dafalias and Taiebat (2013).

To determine λ and κ a linear trendline (equivalent to Equation 3 and Equation 4, respectively) was added to the loading and unloading data sets of isotropic compression test on a NC sample of LCT soil, as shown in Figure 9.

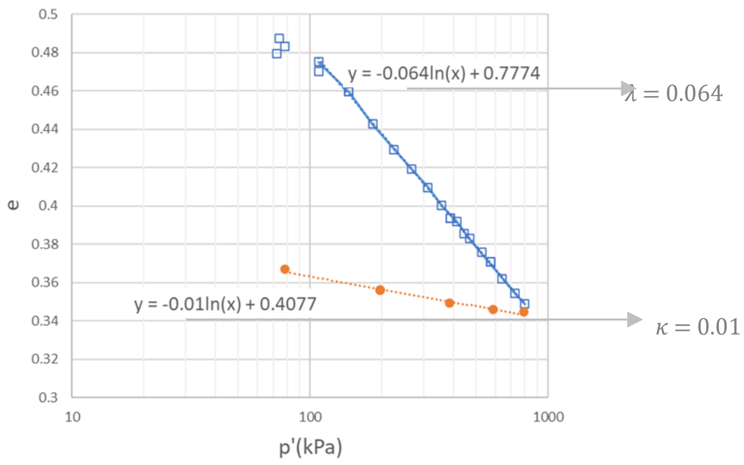

Figure 9. Step 1: determination of λ *and* κ.

To estimate ν, the slope of the initial part of the K0-unloading stress path (Figure 10) is calculated and Equation 6 is used.

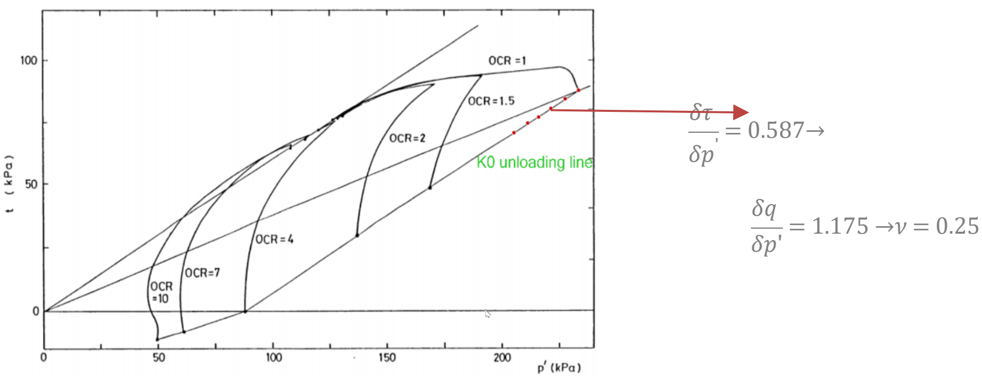

Figure 10. Step 2: determination of the ν (Gens, 1982).

Figure 11 illustrates the test results for undrained triaxial tests performed on K_0-consolidated samples with $OCR = 1$ to 7. These tests ended at around 10% of vertical strain. Looking at the stress-strain graphs of the experimental tests illustrates that the samples did not reach the critical state, although the rate of stress reduction was quite low. Determining M_c and M_e from these data sets might lead to slight overestimation. Using Equation 8 and Equation 9 for compression and extension tests, M_c and M_e would be 1.22 and 0.89, respectively. It is worth noting that the parameters may be estimated simply from the tests on NC samples.

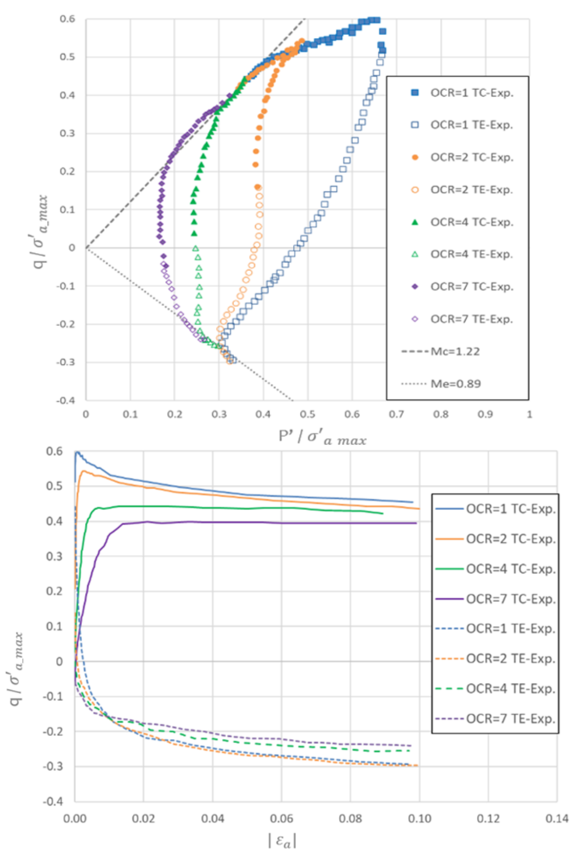

Figure 11. Step 3: determination of the slopes M_c and M_e.

For RH 2006, Equation 10 gives $N = 0.89$. In addition, from Equation 11 to Equation 13, one can obtain $x = 1.71$.

In RH 2013, Equation 16 to Equation 18 lead to $S = Z = 2.23$. Now N_c can be determined from the data of OCR=1 TC set presented on Figure 11. using data of end of consolidation (p'_{K_0},η_{K_0},α_{K_0}) and at critical state (p'_f, M_c,α_c), gives $N_c = 0.92$, hence based on Equation 21 $N_e = 0.67$.

With these values, the parentheses of Equation 22 would have negative value, implying that the Xi parameter would be ignored by SIGMA/W.

Having all the other parameters in hand, one can simulate CK0TE tests on NC samples using SIGMA/W to determine the proper value of parameter C. Refer to the associated GeoStudio example file to configure the simulation. As shown in Figure 12, for each version, three cloned branches analyze the soil response with different values for C. Comparing the results of the stress path and stress-strain plot, in Figure 13 shows that $C = 16$ leads to the best fit in RH 2006.

Back to parameter N of RH 2006, since the calculated value is close to that calculated by Dafalias et al. (2006) ($N = 0.88$), a similar adjustment is proposed, slightly increasing its value to $N = 0.91$. Unfortunately, the model's authors do not propose guidance on how much increase is justified when C is larger than 8. Users are encouraged to verify the sensitivity of their results when varying N.

Similarly in analyses with RH 2013, one may choose $C = 200$ to continue the simulation. The results of extensional tests show that all tested values for C result in overestimated predictions of stresses at critical state. A question raised here is to what extend C affects the compression tests. The results of compression tests in Figure 13 prove that the stress path is not very sensitive to the C value in the tested range, however the predicted stresses at critical state are also higher than the experimental data, clearly for other reasons. As explained previously above Figure 11, it is expected that $M_c = 1.22$ and $M_e = 0.89$ lead to overestimation. It’s worth noting that in RH 2013 M_c and M_e are used to calibrate more parameters, hence the simulation can be more sensitive to their values. Stated that, for the subsequent simulations, the parameters used in RH 2013 have been revised using the M_c and M_e values proposed by Dafalias and Taiebat (2013), as listed in Table 2.

Table 2. Calibrated parameters for the SANICLAY model of LCT.

RH 2006		RH 2013		
Dafalias et al. (2006)	This study	Dafalias et al. (2013)	This study: first trial	This study: revised
λ=0.063	λ=0.064	λ=0.063	λ=0.064	λ=0.064
κ=0.009	κ=0.01	κ=0.009	κ=0.01	κ=0.01
$\nu = 0.2$	$\nu = 0.25$	$\nu = 0.25$	$\nu = 0.25$	$\nu = 0.25$
$M_c = 1.18$	$M_c = 1.22$	$M_c = 1.18$	$M_c = 1.22$	$M_c = 1.18$
$M_e = 0.86$	$M_e = 0.89$	$M_e = 0.86$	$M_e = 0.89$	$M_e = 0.86$
$N = 0.91$	$N = 0.91$	$N_c = 0.8$	$N_c = 0.92$	$N_c = 0.81$
		$N_e = 0.58$	$N_e = 0.67$	$N_e = 0.59$
$x = 1.56$	$x = 1.71$	–	–	–
–	–	$s = 1.72$	$s = 2.23$	$s = 1.76$
–	–	$z = 1.72$	$z = 2.23$	$z = 1.76$
–	–	$Xi = 1.1$	–	$Xi = 1.2$
$C = 16$	$C = 16$	$C = 200$	$C = 200$	$C = 200$
OCR= 1-7	OCR=1-7	OCR= 1-7	OCR= 1-7	OCR= 1-7
$K_{0,nc} = 0.49$	$K_{0,nc} = 0.49$	$K_{0,nc} = 0.49$	$K_{0,nc} = 0.49$	$K_{0,nc} = 0.49$

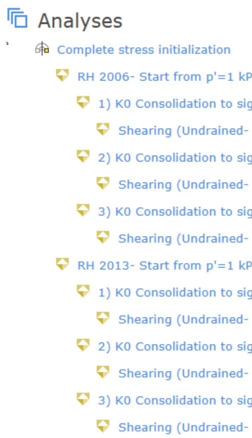

Figure 12. Analysis tree for calibrating parameter C using SIGMA/W.

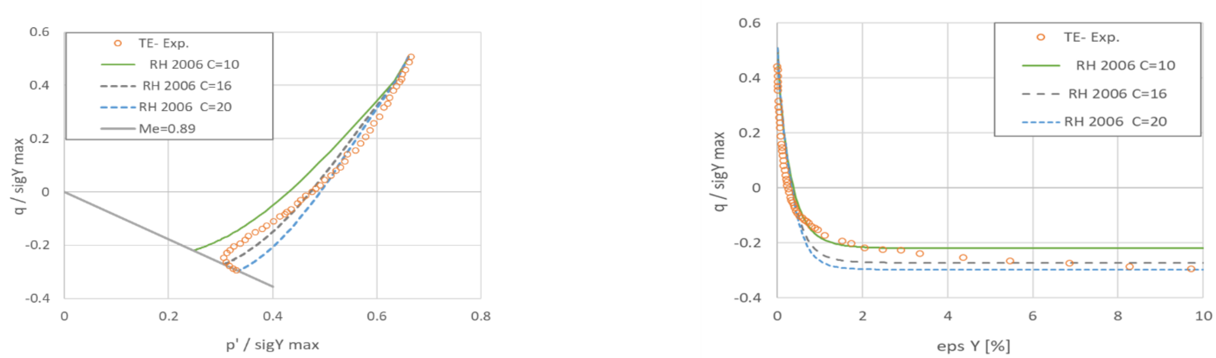

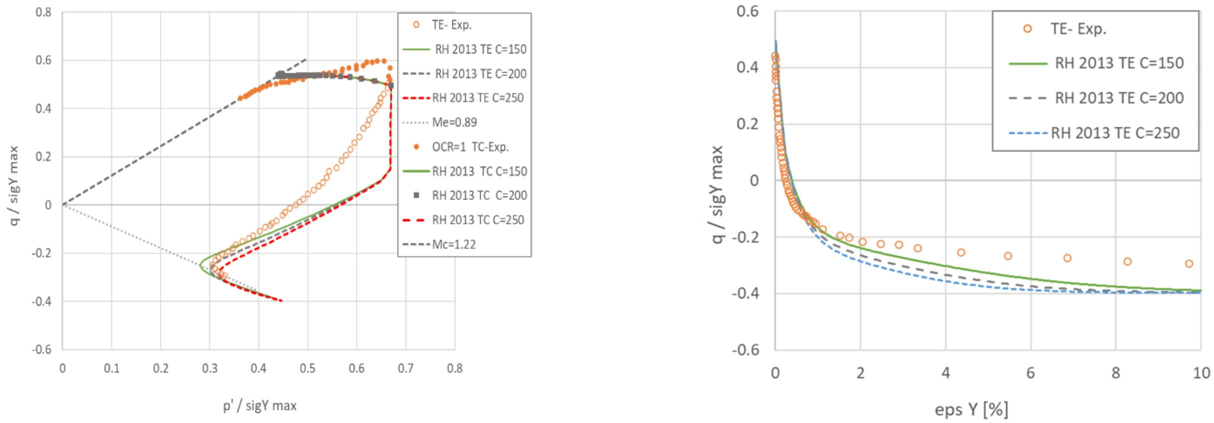

Figure 13. Calibration of parameter C for RH 2006 and RH 2013.

Verification

Figure 14 compares the results obtained from the parameter set defined in this study with the results obtained from the parameter set proposed by Dafalias *et al.* (2006). Beside the numerical simulation results, the measured results by Gens (1982) are also presented. For each OCR, continuous curves and dashed curves are associated with this study and Dafalias *et al.* (2006), respectively. Laboratory data are presented in symbols.

The acceptable consistency between this study and Dafalias *et al.* (2006) indicate the parametrizing steps successfully captured the appropriate values for the parameters of SANICLAY. The slight difference between the two sets of numerical simulation is mainly attributed to the difference in M_c and M_e.

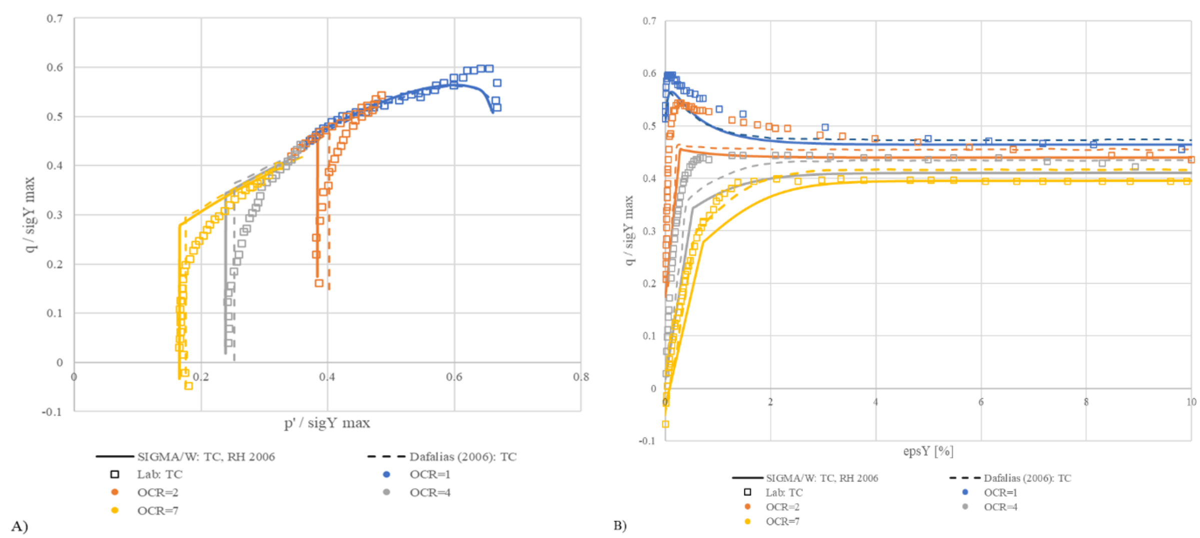

Figure 14. Comparison of results from parameter sets defined in this study (RH 2006) and from the reference paper, alongside laboratory results.

Figure 15 (A and B) presents the results obtained from the revised set of material properties in this study versus the results reported in Dafalias and Taiebat (2013). Again, the promising consistency between this study and Dafalias and Taiebat (2013) indicate the parametrizing steps led to suitable values for the parameters of SANICLAY RH 2013.

Figure 15 (C and D) compares the results obtained from the revised set of material properties in this study with the associated laboratory tests reported by Gens (1982). The acceptable consistency between the laboratory results and simulations indicates the capabilities of the calibrated SANICLAY model in predicting the responses of the clay samples.

To reproduce the simulated results, one can use the GeoStudio example file named Triaxial tests on SANICLAY soil.

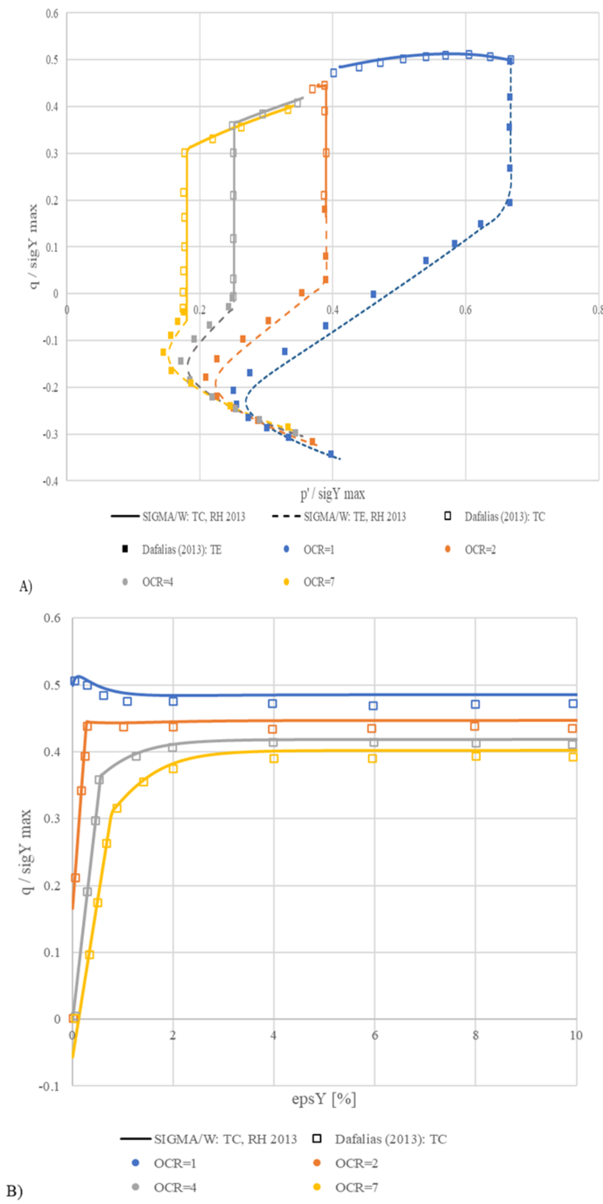

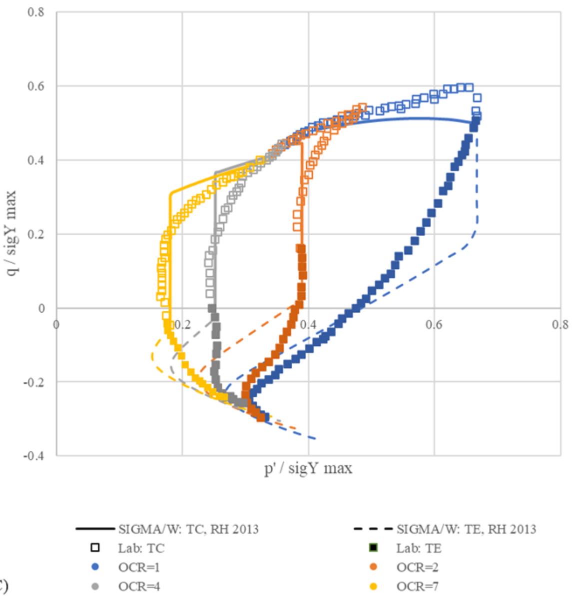

C)

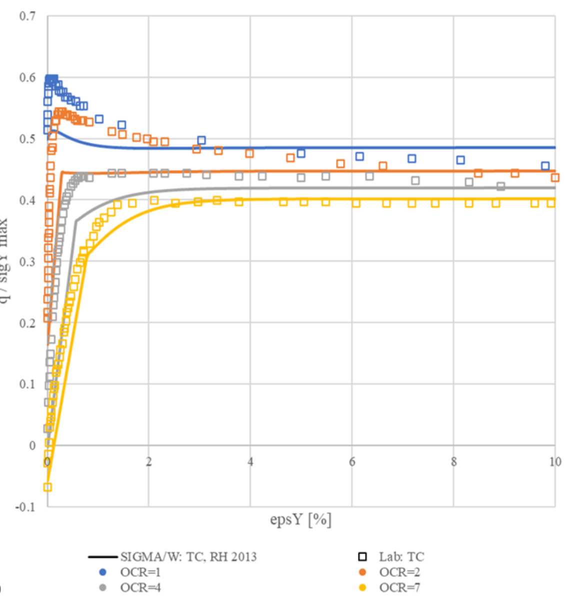

D)

Figure 15. Comparison of results from parameter sets defined in this study (RH 2013) and from the reference paper (A and B), alongside laboratory results (C and D).

Summary

The calibration procedure of the SANICLAY material model for RH 2006 and RH 2013 was provided in six straight forward steps. Results of undrained triaxial tests on K_0-consolidated samples were required for parameterizing the model. The material input parameters were used in numerical simulations and the results were found to compare favorably with both the reference papers (Dafalias et al. (2006) and Dafalias and Taiebat (2013) and the corresponding laboratory results (Gens, 1982).

References

Dafalias, Y.F., Taiebat, M. 2013. Anatomy of rotational hardening in clay plasticity. Geotechnique.63, No. 16, 1406-1418.

Dafalias, Y. F., Manzari, M. T., and Papadimitriou, A. G. 2006. SANICLAY: simple anisotropic clay plasticity model. International Journal for Numerical and Analytical Methods in Geomechanics, 30: 1231-1257.

Gens A. Stress–strain and strength of a low plasticity clay. Ph.D. Thesis, Imperial College, London University, 1983; 856.

Seequent ULC. 2024. Stress-strain modeling with GeoStudio. Calgary, Alberta, Canada.